198639: garnet-bearing psammitic gneiss, Uraloo Bore

(Narryer Terrane, Yilgarn Craton)

Blereau, ER, Korhonen, FJ and Kelsey, DE

Location and sampling

Byro (SG 50-10), Badgeradda (2144)

MGA Zone 50, 395164E 7029983N

WAROX site FJKBGD198639

Sampled on 14 June 2010

This sample was collected from an outcrop west of the Carnarvon–Mullewa Road, about 11.9 km north of Bilga rocks, 5.4 km north-northwest of the Murchison Settlement, and 1.4 km east of Uraloo Bore. The sample was collected as part of the Geological Survey of Western Australia's (GSWA) 2003–14 Yilgarn Craton Metamorphic Project, and referred to in that study as sample BG10-61b. The results from this project have not been released by GSWA, although select data have been published in Goscombe et al. (2019).

Geological context

The unit sampled is a garnet-bearing psammitic gneiss (Fig. 1) of the Narryer Terrane in the northwest Yilgarn Craton (Myers, 1997). The age of the metasedimentary rocks is poorly constrained to between 3050 and 2750 Ma (Nutman et al., 1991; Occhipinti et al., 2001). The Narryer Terrane consists of granitic gneisses and interleaved metasedimentary and mafic meta-igneous rocks that were extensively intruded by sheets of granite and minor gabbro between 2750 and 2620 Ma (Myers, 1990; Nutman et al., 1991). $^{40}Ar/^{39}Ar$ dating of hornblende shows that cooling from amphibolite facies conditions occurred by c. 2700 Ma, prior to the intrusion of fine-grained granite sheets around 2650 Ma (Kinny et al., 1990). Detrital zircons from a mica schist and quartzite about 1.7 km to the east-northeast of this sample, show an age range from 3900 to 2760 Ma for zircon cores and c. 2700 Ma for younger overgrowths (Nutman et al., 1991). Monazite from the sample reported here yielded a weighted mean $^{207}Pb/^{206}Pb$ date of 2723 ± 7 Ma (GSWA 198639, preliminary data), interpreted as the age of metamorphism.

Petrographic description

This sample is a garnet-bearing psammitic gneiss containing about 52% quartz, 33% plagioclase, 11% biotite, 3% garnet, 1% muscovite, trace ilmenite, magnetite, K-feldspar, chlorite, and accessory zircon, monazite, and apatite (Fig. 2; Table 1). Centimetre-scale quartzofeldspathic segregations in the hand sample (Fig. 1) are interpreted to be leucosomes. Sillimanite and cordierite were described in outcrop but have not been identified in thin section. The sample has a coarse-grained (up to 2 mm) quartz–plagioclase matrix that exhibits a polygonal granoblastic texture (Fig. 3a,b). Aligned dark brown to straw coloured biotite laths up to 0.8 mm long define a moderate foliation (Figs 2, 3). Garnet occurs as weakly aligned, irregular, rounded to elongate porphyroblasts up to 1 mm long, containing inclusions of quartz, plagioclase, biotite, magnetite and apatite (Fig. 3a). Fine-grained muscovite less than 200 µm in size occurs at plagioclase margins and chlorite occurs on the margins of garnet. Ilmenite forms aligned tabular crystals, up to 0.1 mm long and occurs with biotite. Magnetite is present as equant to elongate (>0.2 mm) grains with biotite and as inclusions or along fractures in garnet porphyroblasts. Rare K-feldspar occurs as thin films and blebs less than 200 µm in size closely associated with biotite (Fig. 3c,d) and plagioclase. Matrix K-feldspar has also been described in a thin section for this sample by Goscombe et al. (2015).

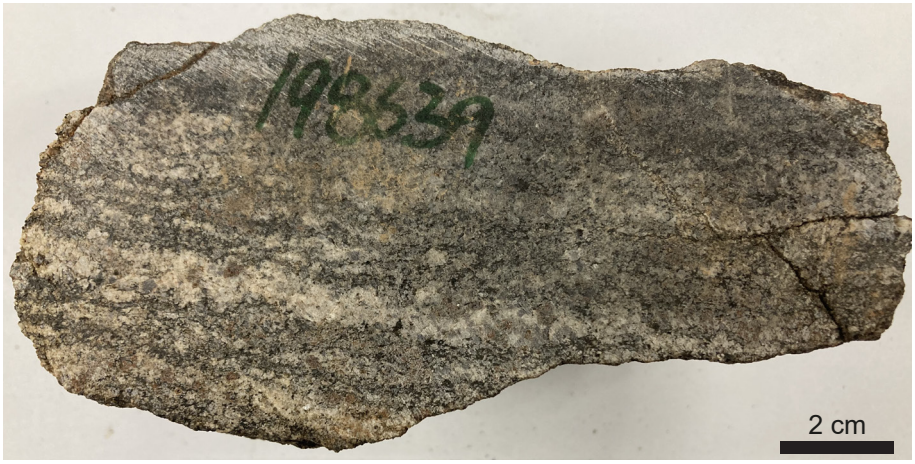

Figure 1. Hand specimen image for sample 198639: garnet-bearing psammitic gneiss, Uraloo Bore

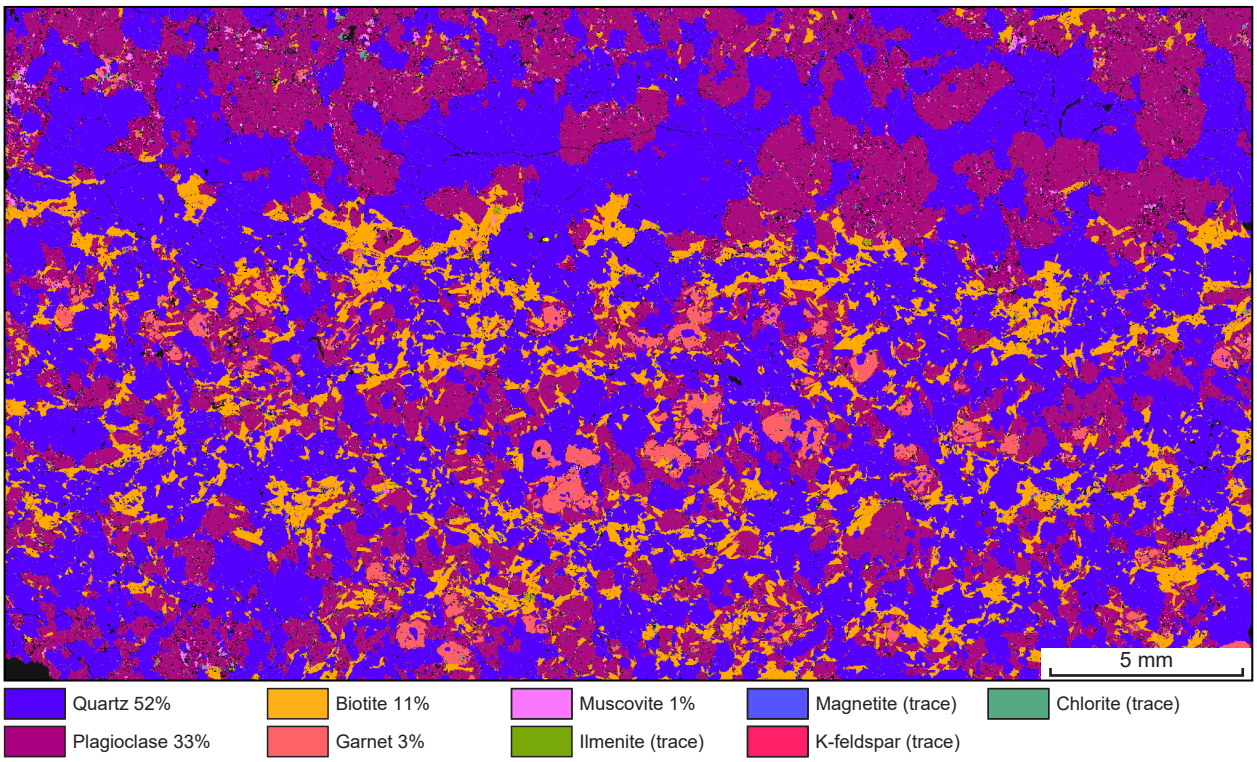

Figure 2. TESCAN Integrated Mineral Analyser (TIMA) image of an entire thin section from sample 198639: garnet-bearing psammitic gneiss, Uraloo Bore. Volume percent proportions of major rock-forming minerals are calculated by the TIMA software

Table 1. Mineral modes for sample 198639: garnet-bearing psammitic gneiss, Uraloo Bore

Mineral modes	Grt	Sil	Bt	Kfs	Ms	Mag	Ilm	Pl	Qz	Liq
Observed (vol%)	3	–	11	–	1	trace	trace	33	52	–
Predicted (mol%)										
@ 5.5 kbar, 735 °C	4.4	1.8	13.4	3.6	–	0.6	1.0	30.7	44.2	0.4
@ 5.5 kbar, 780 °C	12.2	0.1	3.0	9.9	–	0.5	1.5	26.2	39.1	7.7
@ 4.4 kbar, 750 °C	5.9	1.4	11.0	4.9	–	0.9	0.9	29.8	43.0	2.2
@ 4.4 kbar, 750 °C	9.2	1.0	7.7	7.3	–	0.1	1.5	28.1	41.6	3.3

NOTES: – not present

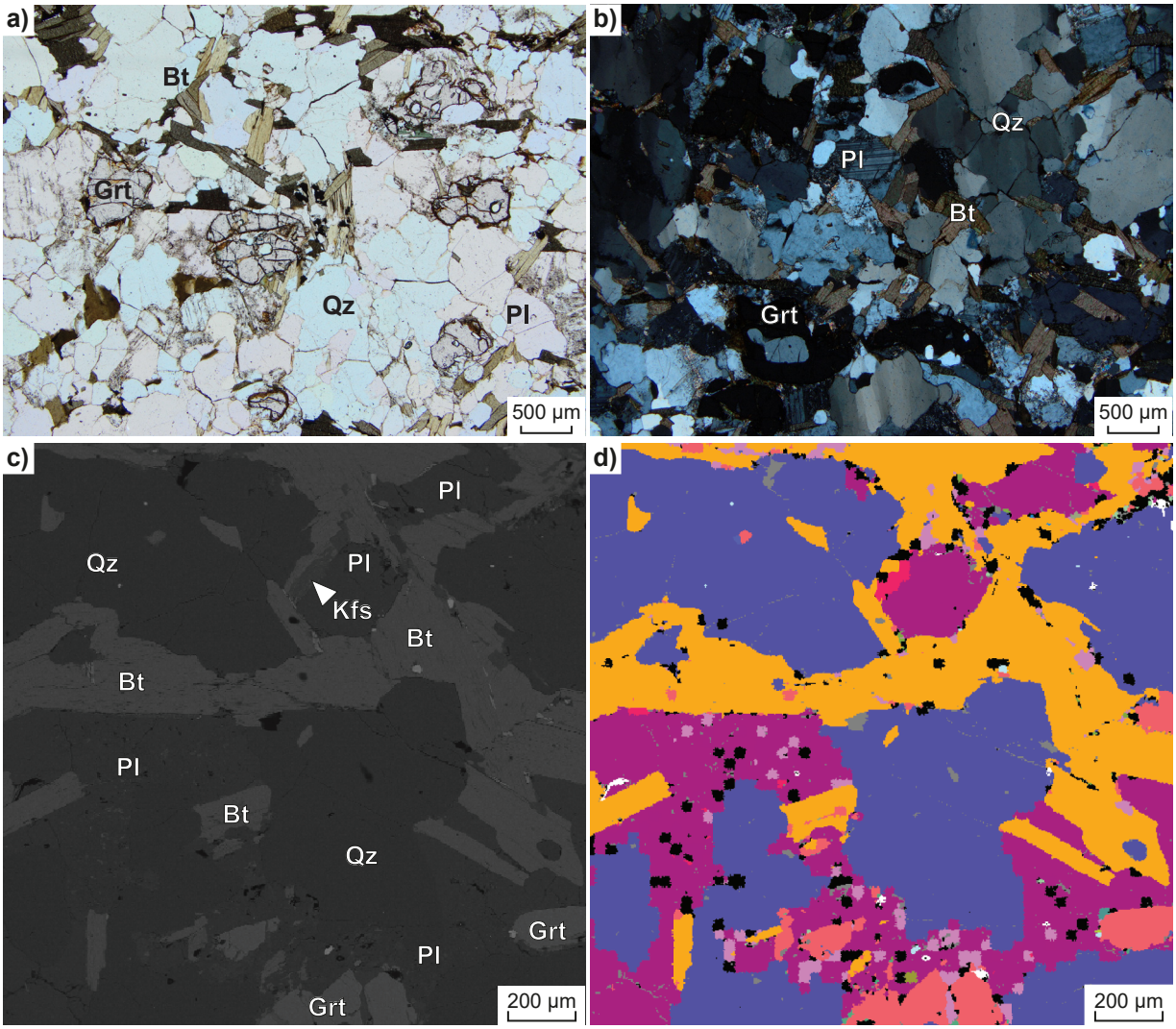

Figure 3. **Thin of sample 198639: garnet-bearing psammitic gneiss, Uraloo Bore: a) photomicrographs in plane-polarized light; b) cross-polarized light; c) backscattered electron image; white arrow points to film of K-feldspar between biotite and plagioclase; d) TIMA image of (c); see Figure 2 for mineral legend, black pixels denote unclassified minerals, white pixels are holes. Abbreviations: Bt, biotite; Grt, garnet; Kfs, K-feldspar; Pl, plagioclase; Qz, quartz**

Analytical details

The metamorphic evolution of this sample has been investigated using phase equilibria modelling, based on the bulk-rock composition (Table 2). The composition was determined by X-ray fluorescence spectroscopy, together with loss on ignition (LOI). The modelled O content (for Fe^{3+}) was set to be 20% of the measured total Fe in order to stabilize the Fe–Ti oxide mineralogy of the sample. The H_2O content is the measured amount of LOI. The bulk composition was corrected for the presence of apatite by applying a correction to calcium (Table 2). Thermodynamic calculations were performed in the MnNCKFMASHTO ($MnO–Na_2O–CaO–K_2O–FeO–MgO–Al_2O_3–SiO_2–H_2O–TiO_2–O$) system using THERMOCALC version tc340 (updated October 2013; Powell and Holland, 1988) and the internally consistent thermodynamic dataset of Holland and Powell (2011; dataset tc-ds62, created in February 2012). The activity–composition relations used in the modelling are detailed in White et al. (2014a,b). Compositional and mode isopleths for all phases were calculated using the software TCInvestigator (Pearce et al., 2015). Additional information on the workflow with relevant background and methodology are provided in Korhonen et al. (2020).

Table 2. Measured whole-rock and modelled compositions for sample 198639: garnet-bearing psammitic gneiss, Uraloo Bore

XRF whole-rock composition (wt%)[a]											
SiO_2	**TiO_2**	**Al_2O_3**	**Fe_2O_3**[b]	**FeO**[b]	**MnO**	**MgO**	**CaO**	**Na_2O**	**K_2O**	**P_2O_5**	**LOI**	**Total**
68.10	0.76	12.30	–	7.79	0.16	1.18	1.96	2.38	2.05	0.14	0.47	97.29
Normalized composition used for phase equilibria modelling (mol%)												
SiO_2	**TiO_2**	**Al_2O_3**	**O**[c]	**FeO^T**[d]	**MnO**	**MgO**	**CaO**[e]	**Na_2O**	**K_2O**	–	**H_2O**[f]	**Total**
74.55	0.63	7.93	0.64	6.41	0.15	1.93	2.08	2.53	1.43		1.72	100

NOTES: (a) Data and analytical details are available from Goscombe et al. (2019)
(b) FeO content is total Fe
(c) O content (for Fe_2O_3) set to be 20% of measured FeO[b]
(d) FeO^T = moles FeO + 2 * moles O
(e) CaO modified to remove apatite: CaO(Mod) = CaO(Total) - (moles CaO(in Ap) = 3.33 * moles P_2O_5)
(f) H_2O content is the measured LOI

Results

Metamorphic *P–T* estimates have been derived based on detailed examination of the thin section and the bulk-rock composition (Table 2). The *P–T* pseudosection for this sample was calculated over a *P–T* range of 2–10 kbar and 600–900 °C (Fig. 4). The solidus is located between 720 and 740 °C across the range of modelled pressures. Garnet and K-feldspar are stable across the entire modelled *P–T* range. Magnetite has a maximum pressure stability of 7.5 kbar, and cordierite has a maximum pressure stability of 5.3 kbar. Aluminosilicate-free assemblages are stable at lower pressures, just below the appearance of cordierite, and above 785 °C. Biotite has a maximum temperature stability of 810 °C at 4.2 kbar. Muscovite is predicted in the high pressure–low temperature part of the diagram, and orthopyroxene is predicted at low pressure–high temperature.

Mineral compositions are provided in Table 3. Garnet porphyroblasts are almandine-rich with Mn-rich and Mg-poor rims. Compositional maps show very little zoning (Appendix 1), but quantitative data indicate a decrease in the proportion of almandine (= Fe^{2+}/[Fe^{2+} + Mg + Ca + Mn]), pyrope (= Mg/[Fe^{2+} + Mg + Ca + Mn]) and grossular (= Ca/[Fe^{2+} + Mg + Ca + Mn]), and an increase in XFe (= Fe^{2+}/[Fe^{2+} + Mg]) and spessartine (= Mn/[Fe^{2+} + Mg + Ca + Mn]) from core to rim. Garnet cores have XFe = 0.90, p(Alm) = 0.81, p(Grs) = 0.07, and p(Sps) = 0.04; rims have XFe = 096; p(Alm) = 0.78, p(Grs) = 0.06, and p(Sps) = 0.13. Plagioclase compositions have Ca(Pl) (= Ca/[Ca + Na + K]) values of 0.30 – 0.31. Biotite compositions have XFe contents of 0.74 – 0.75 and Ti contents of 0.15 – 0.17 per formula unit (pfu).

Interpretation

Based on the coarse grain size and mineral associations that support textural equilibrium, the peak granulite-grade metamorphic assemblage is interpreted to contain garnet, biotite, magnetite, ilmenite, quartz, plagioclase and melt. K-feldspar is predicted across the range of modelled *P–T* conditions, with the predicted abundance decreasing with decreasing temperature. At conditions just above the solidus, a small amount of sillimanite (<2 mol%, approximately equivalent to vol%) is also predicted (Table 1; Appendix 2). A small amount of K-feldspar is observed in thin section (Fig. 3c,d), and its occurrence as films and blebs associated with biotite indicate that it is likely related to biotite dehydration melting. No sillimanite is observed in the thin section, although it is described by Goscombe et al. (2015) at the outcrop for this sample. Based on these observations, the peak assemblage is inferred to be garnet–biotite–K-feldspar–plagioclase–quartz–ilmenite–magnetite–melt±sillimanite.

The garnet–sillimanite–biotite–K-feldspar–plagioclase–quartz–ilmenite–magnetite–melt field is stable between 720 and 785 °C at 3.9 – 7.4 kbar, and the sillimanite-absent field is stable between 780 and 810 °C at 4.4 – 6.7 kbar. With the exception of sillimanite, the predicted mineral modes are most consistent with equilibration in the garnet–sillimanite–biotite–K-feldspar–plagioclase–quartz–ilmenite–magnetite–melt field at conditions just above the solidus (Table 1; Appendix 2). Grossular contents in garnet (= 0.06 – 0.07) indicate equilibration towards the upper pressure limit of the peak assemblage field. Based on these constraints, peak metamorphic conditions are refined to be 720–745 °C and 6.9 – 7.5 kbar (Fig. 4; Appendix 2).

Peak metamorphic conditions are estimated at 6.9 – 7.5 kbar and 720–745 °C, with an apparent thermal gradient between 100 and 105 °C/kbar. There is no information on the prograde segment of the *P–T* path; the possible presence of cordierite in the outcrop described by Goscombe et al. (2015) may indicate post-peak decompression, although this cannot be verified.

Table 3. Mineral compositions for sample 198639: garnet-bearing psammitic gneiss, Uraloo Bore

Mineral[a]	Ms	Chl	Bt	Grt	Grt	Grt	Grt	Bt	Bt	Pl	Pl
Setting[b]	Core	Core	Incl	Core	Mantle	Rim	OR	Core	Rim	Core	Rim
wt%											
SiO_2	44.25	23.10	34.07	36.64	36.21	36.17	36.12	33.22	33.40	60.57	59.83
TiO_2	1.09	0.06	2.48	0.02	0.00	0.01	0.00	2.72	2.77	0.00	0.01
Al_2O_3	31.79	21.07	17.59	20.98	20.84	20.91	20.92	17.43	17.75	24.91	25.15
Cr_2O_3	0.02	0.01	0.00	0.04	0.00	0.00	0.01	0.04	0.05	0.00	0.00
FeO	6.50	34.62	27.05	36.47	36.13	35.59	34.06	26.58	26.42	0.05	0.04
MnO	0.04	0.17	0.10	1.72	2.00	3.98	5.60	0.08	0.09	0.00	0.01
MgO	1.07	8.00	5.08	2.11	1.92	1.08	0.69	4.80	4.79	0.00	0.00
ZnO	0.07	0.09	0.00	0.00	0.00	0.02	0.19	0.13	0.00	0.00	0.07
CaO	0.00	0.01	0.04	2.28	2.26	2.04	2.03	0.00	0.06	6.36	6.64
Na_2O	0.28	0.00	0.18	0.00	0.00	0.05	0.00	0.11	0.08	8.00	8.06
K_2O	9.90	0.04	9.09	0.00	0.01	0.02	0.00	9.32	8.57	0.14	0.07
Total[c]	95.00	87.18	95.68	100.27	99.37	99.88	99.60	94.44	93.97	100.03	99.87
Oxygen	11	14	11	12	12	12	12	11	11	8	8
Si	3.01	2.56	2.68	2.96	2.96	2.96	2.97	2.66	2.67	2.69	2.66
Ti	0.06	0.00	0.15	0.00	0.00	0.00	0.00	0.16	0.17	0.00	0.00
Al	2.55	2.76	1.63	2.00	2.01	2.01	2.03	1.64	1.67	1.30	1.32
Cr	0.00	0.00	0.00	0.00	0.00	0.00	0.00	0.00	0.00	0.00	0.00
Fe^{3+}[d]	0.21	0.34	0.09	0.07	0.08	0.08	0.04	0.09	0.09	0.00	0.00
Fe^{2+}	0.16	2.87	1.69	2.39	2.39	2.35	2.30	1.69	1.67	0.00	0.00
Mn^{2+}	0.00	0.02	0.01	0.12	0.14	0.28	0.39	0.01	0.01	0.00	0.00
Mg	0.11	1.32	0.60	0.25	0.23	0.13	0.08	0.57	0.57	0.00	0.00
Zn	0.00	0.01	0.00	0.00	0.00	0.00	0.01	0.01	0.00	0.00	0.00
Ca	0.00	0.00	0.00	0.20	0.20	0.18	0.18	0.00	0.00	0.30	0.32
Na	0.04	0.00	0.03	0.00	0.00	0.01	0.00	0.02	0.01	0.69	0.70
K	0.86	0.01	0.91	0.00	0.00	0.00	0.00	0.95	0.87	0.01	0.00
Total	5.00	5.00	5.00	5.00	8.00	8.00	8.00	7.60	7.59	7.61	4.00
Compositional variables[e]											
Ca(Pl)	–	–	–	–	–	–	–	–	–	0.30	0.31
p(Alm)	–	–	–	0.81	0.81	0.80	0.78	–	–	–	–
p(Prp)	–	–	–	0.05	0.04	0.00	0.01	–	–	–	–
p(Grs)	–	–	–	0.07	0.07	0.06	0.06	–	–	–	–
p(Sps)	–	–	–	0.04	0.05	0.09	0.13	–	–	–	–
XFe	0.60	0.68	0.74	0.90	0.91	0.95	0.96	0.75	0.75	–	–

NOTES: – not applicable
(a) Mineral abbreviations explained in the caption to Figure 4
(b) OR, outer rim
(c) Totals on anhydrous basis
(d) Fe^{3+} contents for biotite assumed to be 10% of Fe total; Fe^{3+} contents for other minerals based on Droop (1987)
(e) Ca(Pl) = Ca/(Ca + Na + K);
proportion of almandine, p(Alm) = $Fe^{2+}/(Fe^{2+} + Mg + Mn + Ca)$;
proportion of pyrope, p(Prp) = $Mg/(Fe^{2+} + Mg + Mn + Ca)$;
proportion of grossular, p(Grs) = $Ca/(Fe^{2+} + Mg + Mn + Ca)$;
proportion of spessartine, p(Sps) = $Mn/(Fe^{2+} + Mg + Mn + Ca)$;
XFe = $Fe^{2+}/(Fe^{2+} + Mg)$

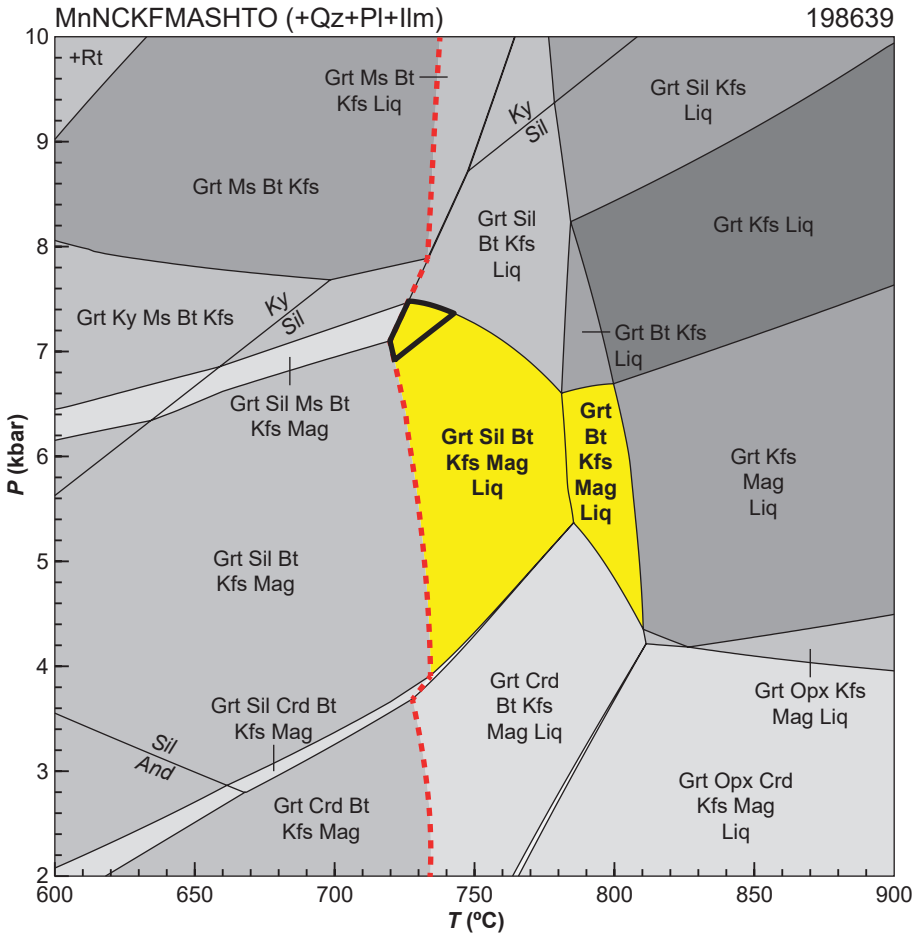

Figure 4. ***P–T*** **pseudosection calculated for sample 198639: garnet-bearing psammitic gneiss, Uraloo Bore. Assemblage field corresponding to peak metamorphic conditions is shown in bold text and yellow shading. Red dashed line represents the solidus. Thick black lines delimit estimated peak conditions (see Appendix 2, text). Abbreviations: And, andalusite; Bt, biotite; Crd, cordierite; Grt, garnet; Ilm, ilmenite; Kfs, K-feldspar; Ky, kyanite; Liq, silicate melt; Mag, magnetite; Opx, orthopyroxene; Pl, plagioclase; Qz, quartz; Rt, rutile; Sil, sillimanite**

References

Droop, GTR 1987, A general equation for estimating Fe^{3+} concentrations in ferromagnesian silicates and oxides from microprobe analyses, using stoichiometric criteria: Mineralogical Magazine, v. 51, no. 361, p. 431–435, doi:10.1180/minmag.1987.051.361.10.

Goscombe, B, Blewett, R, Groenewald, PB, Foster, D, Wade, B, Wyche, S, Wingate, MTD and Kirkland, CL 2015, Metamorphic Evolution of the Yilgarn Craton: Geological Survey of Western Australia (unpublished), 910p.

Goscombe, B, Foster, DA, Blewett, R, Czarnota, K, Wade, B, Groenewald, B and Gray, D 2019, Neoarchaean metamorphic evolution of the Yilgarn Craton: a record of subduction, accretion, extension and lithospheric delamination: Precambrian Research, v. 335, doi:10.1016/j.precamres.2019.105441.

Holland, TJB and Powell, R 2011, An improved and extended internally consistent thermodynamic dataset for phases of petrological interest, involving a new equation of state for solids: Journal of Metamorphic Geology, v. 29, no. 3, p. 333–383.

Kinny, PD, Wijbrans, JR, Froude, DO, Williams, IS and Compston, W 1990, Age constraints on the geological evolution of the Narryer Gneiss Complex, Western Australia: Australian Journal of Earth Sciences, v. 37, no. 1, p. 51–69, doi:10.1080/08120099008727905.

Korhonen, FJ, Kelsey, DE, Fielding IOH and Romano, SS 2020, The utility of the metamorphic rock record: constraining the pressure–temperature–time conditions of metamorphism: Geological Survey of Western Australia, Record 2020/14, 24p.

Myers, JS 1990, Narryer Geniss Complex: Part 1: Summary of the Narryer Gneiss Complex, *in* Excursion guidebook: Third International Archaean Symposium, Perth 1990 (17–21 September) *edited by* SE Ho, JE Glover, JS Myers and JR Muhling: The University of Western Australia, Geology Department and University Extension, Publication 21, p. 62–71.

Myers, JS 1997, Byro, WA, Sheet SG 50-10 (2nd edition): Western Australia Geological Survey, 1:250 000 Geological Series.

Nutman, AP, Kinny, PD, Compston, W and Williams, IS 1991, SHRIMP U–Pb zircon geochronology of the Narryer Gneiss Complex, Western Australia: Precambrian Research, v. 52, p. 275–300.

Occhipinti, SA, Sheppard, S, Myers, JS, Tyler, IM and Nelson, DR 2001, Archaean and Palaeoproterozoic geology of the Narryer Terrane (Yilgarn Craton) and the southern Gascoyne Complex (Capricorn Orogen), Western Australia — a field guide: Geological Survey of Western Australia, Record 2001/8, 70p.

Pearce, MA, White, AJR and Gazley, MF 2015, TCInvestigator: automated calculation of mineral mode and composition contours for thermocalc pseudosections: Journal of Metamorphic Geology, v. 33, no. 4, p. 413–425, doi:10.1111/jmg.12126.

Powell, R and Holland, TJB 1988, An internally consistent dataset with uncertainties and correlations: 3. Applications to geobarometry, worked examples and a computer program: Journal of Metamorphic Geology, v. 6, no. 2, p. 173–204.

White, RW, Powell, R, Holland, TJB, Johnson, TE and Green, ECR 2014a, New mineral activity-composition relations for thermodynamic calculations in metapelitic systems: Journal of Metamorphic Geology, v. 32, no. 3, p. 261–286.

White, RW, Powell, R and Johnson, TE 2014b, The effect of Mn on mineral stability in metapelites revisited: New a–x relations for manganese-bearing minerals: Journal of Metamorphic Geology, v. 32, no. 8, p. 809–828.

Appendix 1

EPMA compositional maps of garnet from sample 198639: garnet-bearing psammitic gneiss, Uraloo Bore. Maps were analysd by energy-dispersive spectroscopy (EDS), and show relative elemental abundances. These garnet porphyroblasts were analysed from a thin section of the sample that is not part of the GSWA collection, and as such there is no information on mineral size or petrographic context; from Goscombe et al. (2015)

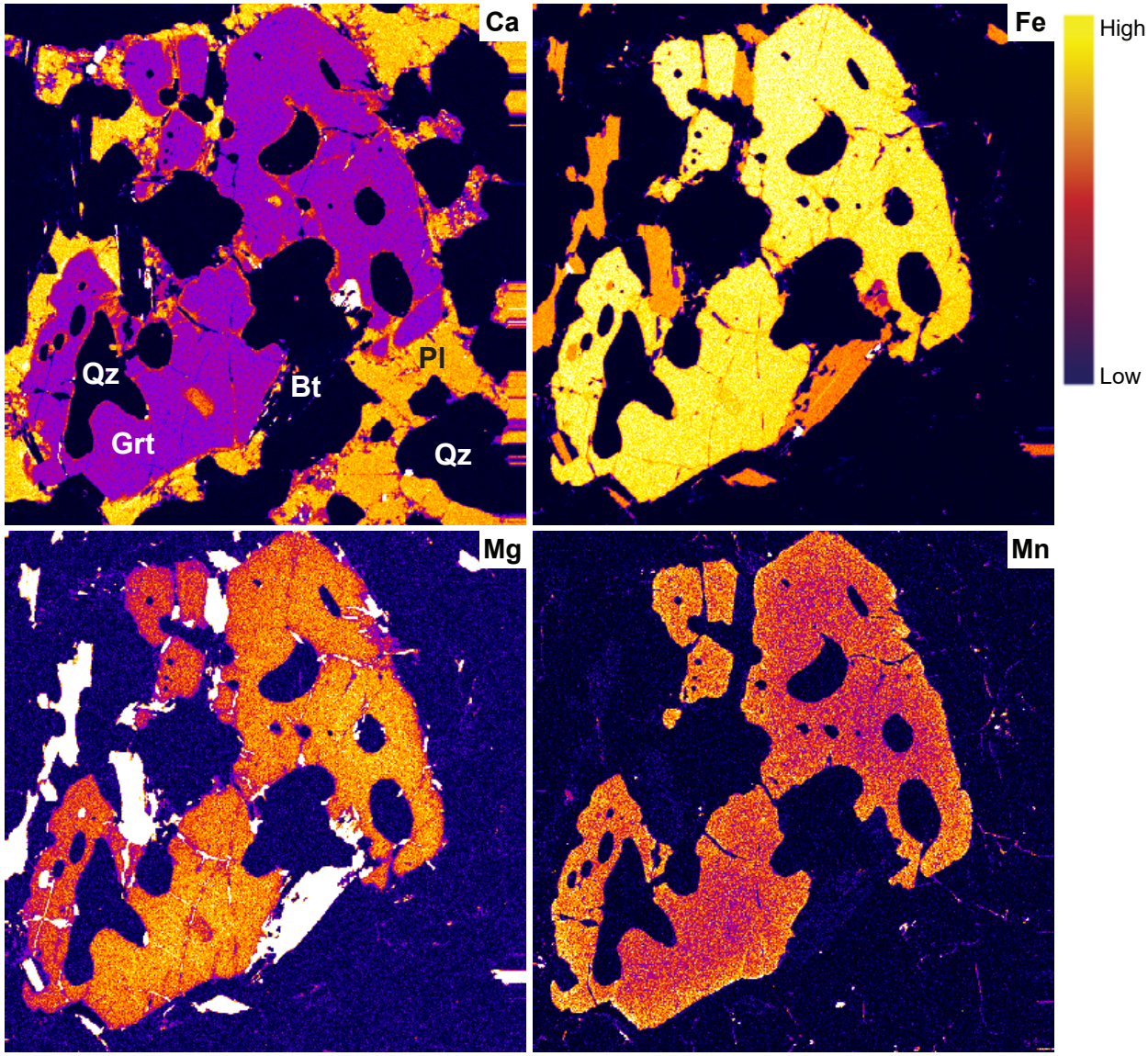

Appendix 2

Compositional and mode (mineral proportions; approximately equal to volume percent) and isopleths for selected minerals in sample 198639: garnet-bearing psammitic gneiss, Uraloo Bore. Labelled *P–T* diagram provided in Figure 4. Garnet compositions — p(Grs) = 0.06 – 0.07 — and mineral modes are most consistent with equilibration in the higher pressure part of the peak assemblage field (thick black lines); see text

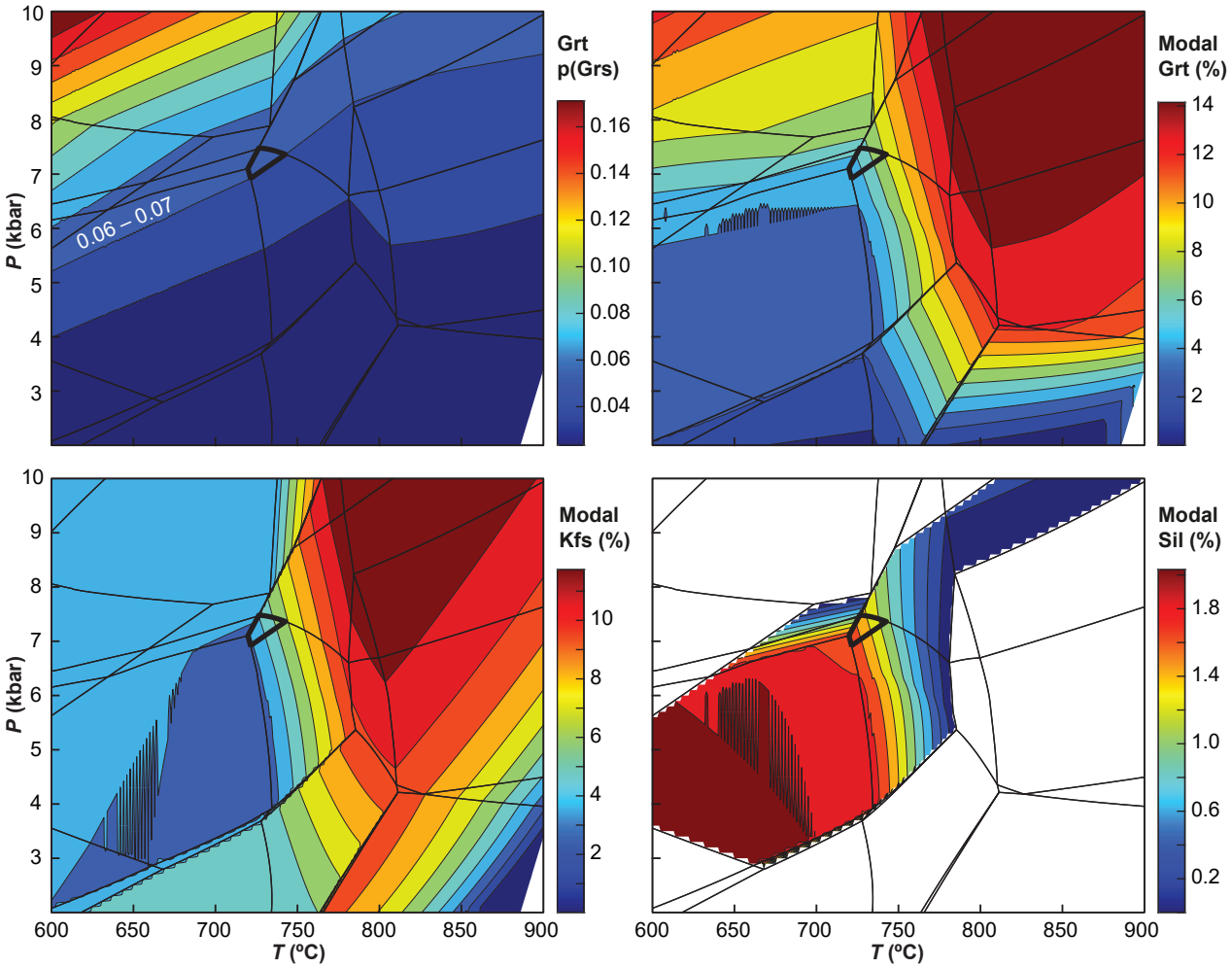

Links

Record 2020/14 The utility of the metamorphic rock record: constraining the pressure–temperature–time conditions of metamorphism

Recommended reference for this publication

Blereau, ER, Korhonen, FJ and Kelsey, DE, 198639: garnet-bearing psammitic gneiss, Uraloo Bore; Metamorphic History Record 24: Geological Survey of Western Australia, 9p.

Data obtained: 28 August 2019

Date released: 7 October 2022

This Metamorphic History Record was last modified on 5 October 2022

Grid references in this publication refer to the Geocentric Datum of Australia 1994 (GDA94). All locations are quoted to at least the nearest 100 m.

WAROX is GSWA's field observation and sample database. WAROX site IDs have the format 'ABCXXXnnnnnnSS', where ABC = geologist username, XXX = project or map code, nnnnnn = 6 digit site number, and SS = optional alphabetic suffix (maximum 2 characters).

Isotope and element analyses are routinely conducted using the GeoHistory laser ablation ICP-MS and Sensitive High-Resolution Ion Microprobe (SHRIMP) ion microprobe facilities at the John de Laeter Centre (JdLC), Curtin University, with the financial support of the Australian Research Council and AuScope National Collaborative Research Infrastructure Strategy (NCRIS). The TESCAN Integrated Mineral Analyser (TIMA) instrument was funded by a grant from the Australian Research Council (LE140100150) and is operated by the JdLC with the support of the Geological Survey of Western Australia, The University of Western Australia (UWA) and Murdoch University. Mineral analyses are routinely obtained using the electron probe microanalyser (EPMA) facilities at the Centre for Microscopy, Characterisation and Analysis, UWA, at Adelaide Microscopy, University of Adelaide, and at the Electron Microscopy and X-ray Microanalysis Facility, University of Tasmania.

Digital data related to WA Geology Online, including geochronology and digital geology, are available online at the Department's Data and Software Centre and may be viewed in map context at GeoVIEW.WA.

Further details of geoscience products are available from:
Information Centre
Department of Mines, Industry Regulation and Safety
100 Plain Street
EAST PERTH WA 6004
Telephone: +61 8 9222 3459 | Email: publications@dmirs.wa.gov.au
www.dmirs.wa.gov.au/GSWApublications